

Constraints on the Dark Energy from the holographic connection to the small l CMB Suppression

Jianyong Shen, Bin Wang*

*Department of Physics, Fudan University,
Shanghai 200433, People's Republic of China*

Elcio Abdalla†

*Instituto de Fisica, Universidade de Sao Paulo,
C.P.66.318, CEP 05315-970, Sao Paulo, Brazil*

Ru-Keng Su‡

*China Center of Advanced Science and Technology (World Laboratory),
P.B.Box 8730, Beijing 100080, People's Republic of China
Department of Physics, Fudan University,
Shanghai 200433, People's Republic of China*

Abstract

Using the recently obtained holographic cosmic duality, we reached a reasonable quantitative agreement between predictions of the Cosmic Microwave Background Radiation at small l and the WMAP observations, showing the power of the holographic idea. We also got constraints on the dark energy and its behaviour as a function of the redshift upon relating it to the small l CMB spectrum. For a redshift independent dark energy, our constraint is consistent with the supernova results, which again shows the correctness of the cosmic duality prescription. We have also extended our study to the redshift dependence of the dark energy.

PACS numbers: 98.80.Cq, 98.80.-k

*Electronic address: wangb@fudan.edu.cn

†Electronic address: eabdalla@fma.if.usp.br

‡Electronic address: rksu@fudan.ac.cn

The latest version of the standard cosmological model describes an infinite flat universe forever expanding under the pressure of dark energy. The first year data from the Wilkinson Microwave Anisotropy Probe (WMAP) manifests a striking agreement with this model [1]. However, as originally discovered by the COBE satellite project, WMAP results imply a suppression of the Cosmic Microwave Background Radiation (CMB) anisotropy power on the largest angular scale as compared to the standard model prediction. Researchers are now seeking an explanation of such a wide-angle missing power in the CMB observation [2]-[5].

Recently, an intriguing attempt to relate the suppression of CMB power in low multipoles to the holographic idea was put forward [6]. The holographic reasoning emerged first in the context of black holes [7] and later got extended to the cosmological setting [8], having attracted a lot of attention in the past decade [9]-[13]. It is viewed as a real conceptual change in our thinking about gravity [14]. There are many applications of holography to the study of cosmology, such as the question of the cosmological constant [15], selecting physical models in inhomogeneous cosmology [12], putting an upper bound on the number of e-foldings in inflation [16] and investigating questions related to dark energy [17][18]. A holographic interpretation of the features concerned with low multipoles in the CMB power spectrum [6] is one more example of how holography can be a useful tool in understanding cosmology.

A finite universe could be the consequence of a holographic constraint, giving rise to an effective IR cutoff. In [6], the relation between the features at low multipoles in the CMB power spectrum and the equation of state of the dark energy was built through a cosmic IR/UV duality between a global infrared cutoff and the ultra violet cutoff. In such a cosmic duality model, the qualitative low l CMB features could be well described.

In this paper we employ the disclosed cosmic duality to study the nature of the dark energy from the WMAP experimental data for the small l CMB power spectrum. For a redshift independent equation of state for the dark energy, the result revealed from the correlation to the observational power spectrum supports the holographic dark energy model [17]. We will also investigate the evolution of dark energy from the CMB observation in the low multipoles.

Starting from the holographic idea relating the UV and IR cutoffs as suggested in [19], the dark energy density in a flat universe is [17]

$$\rho_{\Lambda} = 3c^2 M_p^2 L^2 \quad , \quad (1)$$

where L is the IR cutoff, c is a free parameter satisfying $c \geq 1$ as a consequence of the second law of thermodynamics [17]. Using definitions $\Omega_{\Lambda} = \rho_{\Lambda}/\rho_{cr}$ with $\rho_{cr} = 3M_p^2 H^2$, we have at the present epoch the IR cutoff $L = \frac{c}{\sqrt{\Omega_{\Lambda}^0} H_0}$. Interpreting the IR cutoff L as a cutoff of the physical

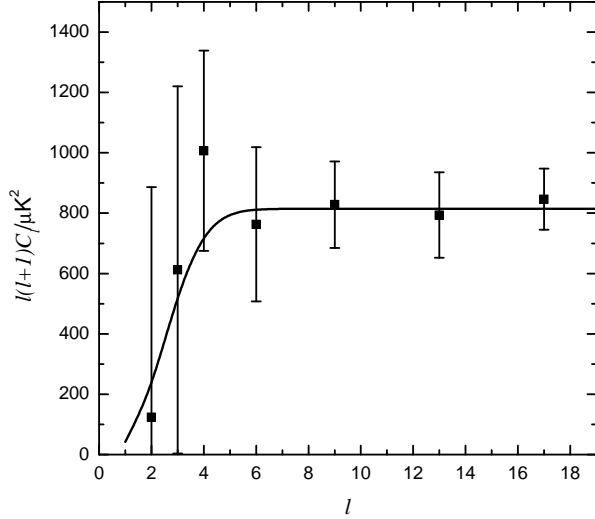


Figure 1: The angular power spectrum at low l . The solid curve stands for the best fit and the square points for the experimental data from WMAP.

wavelength, we have $\lambda_c = 2L$ [6]. Thus the smallest wave number at present is $k_c = \frac{\pi}{c} \sqrt{\Omega_\Lambda^0} H_0$.

The IR cutoff would show up in the CMB angular spectrum in the Sachs-Wolfe effect,

$$C_l = \frac{2\pi}{25} \int_{k_c}^{\infty} \frac{dk}{k} j_l^2(k(\eta_0 - \eta_*)) P_R(k), \quad (2)$$

where $P_R = Ak^{n_s-1}$ is the curvature power spectrum in the flat universe, A is the amplitude, j_l is the Bessel function and $\eta_0 - \eta_*$ is the comoving distance to the last scattering which follows from the definition of comoving time,

$$\eta_0 - \eta_* = \int_0^{z_*} \frac{dz'}{H(z')} \quad . \quad (3)$$

Assuming that the dominant components of energy in the universe are dark energy and matter, then

$$H^2(z) = H_0^2 [(1 - \Omega_\Lambda^0)(1+z)^3 + \Omega_\Lambda^0 f(z)] \quad , \quad (4)$$

where $f(z) = \exp\{3 \int_0^z \frac{1+\omega(z')}{1+z'} dz'\}$ [20]. For a redshift independent equation of state $\omega = \text{const.}$, $f(z) = (1+z)^{3(1+\omega)}$. The distance to the last scattering depends on ω , which on its turn enters the Sachs-Wolfe effect expression (2). Thus the relative position of the cutoff in the CMB spectrum depends on the equation of state of dark energy. This exhibits the CMB/Dark Energy cosmic duality first realized in [6], that is, there is a correlation between CMB and the form of the equation of state for the dark energy. We now will use such a duality to get information on the dark energy from the observed features about the small l CMB spectrum.

Our first attempt is to focus on the case of a redshift independent equation of state of the dark energy. Using Eqs.(2)-(4) to fit the WMAP observational data at low l multipoles [1], we have three parameters, namely (c, ω, A) to be determined. The best fitting result of these parameters are determined by the minimum value of $\sigma = \sum_i [y(l_i) - y_i]^2$, where $y(l_i) = l_i(l_i+1)C_{l_i}$ is computed by Eq.(2) and y_i is the observational data from WMAP at different multipoles. In this numerical analysis, we have taken $z_* = 1100$, $\Omega_\Lambda^0 = 0.7$ and $n_s = 1$. The fitting result is shown in Fig.1 with the position of the cutoff $l_c \sim 4$. It describes the low l CMB features extremely well. The quantitative agreement with the WMAP observation gives further support to the holographic cosmic duality.

The best fitting result determines $c = 2.1$. The value of c bigger than unit obtained from the small l CMB data fitting gives further support to the thermodynamical argumentation discussed in [17].

The equation of state of dark energy ω is determined from the fitting to WMAP data at low multipoles by using the cosmic duality. By minimizing σ , we find $\omega = -0.7$ with minimum value σ_{min} . In the vicinity of $\omega = -0.7$, we observed that differences of corresponding σ 's are small. Imposing the criterion $\frac{\sigma - \sigma_{min}}{\sigma_{min}} < 10\%$, we obtained the range of $\omega \in [-1.3, -0.6]$, which agrees to the result from supernova[25]. The more precise observational results on the exact location of the cutoff l_c and its CMB data are crucial to constrain the static equation of state of dark energy.

In [17], by identifying the IR cutoff exactly with the future and horizon, the holographic dark energy equation of state is expressed as

$$\omega = -\frac{1}{3} - \frac{2\sqrt{\Omega_\Lambda}}{3c} . \quad (5)$$

Since $c \geq 1$, the phantom case ($\omega < -1$ corresponding to $c < 1$) is excluded. Choosing $\Omega_\Lambda = 0.7$ and $c = 2.1$, Eq.(5) tells us $\omega \approx -0.6$, which is on the border of the range of the fitting result above.

In the study of the cosmic duality model, we see that the IR cutoff plays an important role.

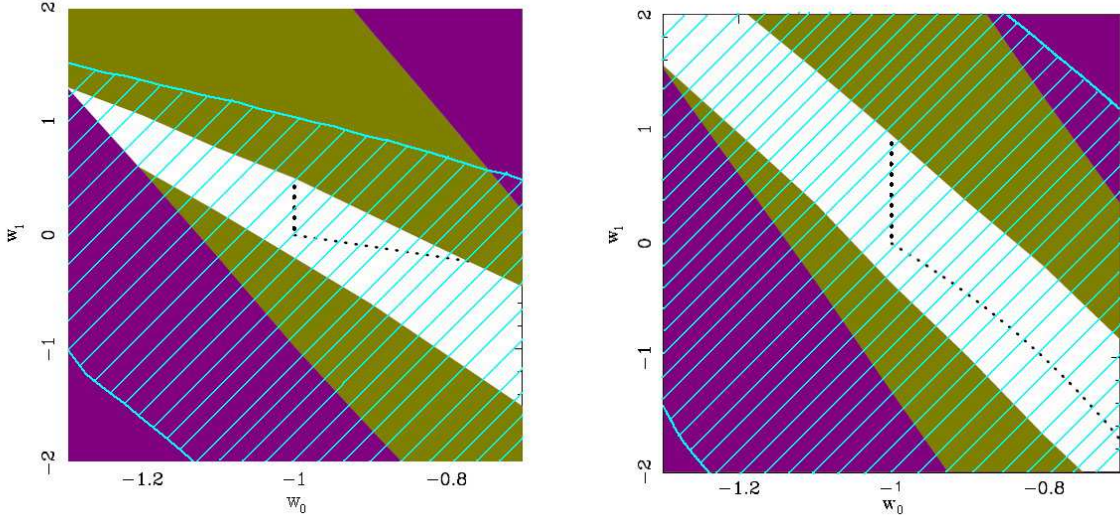


Figure 2: The relations between ω_1 and ω_0 for the model $\omega^I(z)$, Eq.(7), is on the left panel and for $\omega^{II}(z)$, Eq.(8), on the right panel. The purple area is ruled out by Supernova data and the yellow ruled out by WMAP[23]. The shaded area is the holographic constraint from the cosmic duality with the suppression position locates in the interval $4.2 \geq l_c \geq 3.8$.

However, even if an IR/UV duality is at work in the theory at some fundamental level, the IR cutoff can not be simply related to the exact future event horizon. Suppose the IR cutoff has the scale $L = fR_h$, where R_h is the future event horizon $R_h = a \int_t^\infty \frac{dt'}{a(t')}$ and f is just a constant, then the holographic dark energy equation of state

$$\omega = -\frac{1}{3} - \frac{2\sqrt{\Omega_\Lambda}}{3(c/f)}. \quad (6)$$

With the fitting result $c = 2.1$, Eq.(6) allows accommodating $\omega < -1$ case if $f > 2.5$. If $f = 1$, $\omega \approx 0.6$, while $\omega = -1.3$ for $f = 3.6$. We expect that future accurate CMB data at low multipoles can exactly constrain the ω value and in turn help us answering the question of whether the effective IR regulator is of the same magnitude as the measure of the future event horizon.

We now discuss the redshift dependence of ω . We employ three parameterization discussed previously [21]-[25]. The first two are

$$\omega^I(z) = \omega_0 + \omega_1 \frac{z}{1+z} \quad (7)$$

and

$$\omega^{II}(z) = \omega_0 + \omega_1 \frac{z}{(1+z)^2}. \quad (8)$$

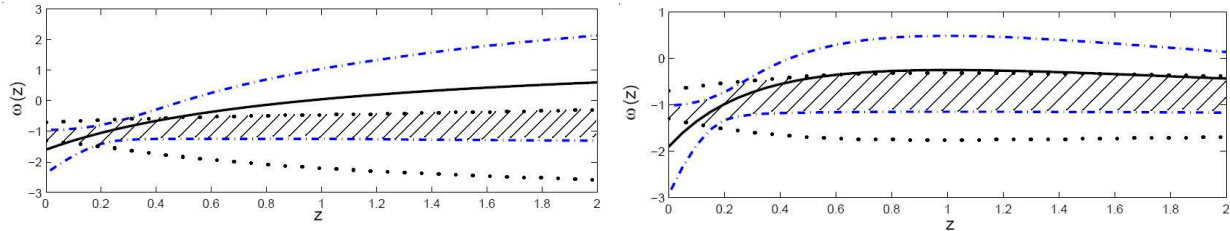


Figure 3: The evolution of the models of $\omega^I(z)$, Eq.(7), is on the left panel and that of $\omega^{II}(z)$, Eq.(8), is on the right panel. The blue dot-dashed lines give the constraints of their evolutions from the supernova observation. The solid black lines stand for the evolutions of golden sets of supernova data[24]. The black dotted lines are obtained from the low l CMB data. The shaded areas are the overlap between supernova and low l CMB observational constraints.

For both cases we have $\omega(0) = \omega_0$, $\omega'(0) = \omega_1$. However, the high redshift behaviours of these functions are different: $\omega(\infty) = \omega_0 + \omega_1$ for Eq.(7) while $\omega(\infty) = \omega_0$ for Eq.(8). Hence Eq.(8) can model a dark energy component which has the same equation of state at the present epoch and at high redshift, with rapid variation at low z . For Eq.(7), we can trust the results only if $\omega_0 + \omega_1$ is well below zero at the time of decoupling.

The third parametrization we will use for the dark energy is called the Taylor expansion model [25]

$$\omega^{III}(z) = \frac{A_1(1+z) + 2A_2(1+z)^2}{3[A_0 + A_1(1+z) + A_2(1+z)^2]} - 1 \quad . \quad (9)$$

The effect of low- l CMB suppression can provide constraints on dynamical models of dark energy. Using Eqs.(2-4) we can obtain the behavior of the variation of ω from the CMB data through cosmic duality. The exact location of the cutoff l_c and the shape of the spectrum at low l are crucial to investigate the redshift dependence of ω . Here we narrow the position of the cutoff l_c in the multipole space in the interval $3.8 < l_c < 4.2$. The free parameter c is set to be 2.1.

Fig.2 exhibits the constraints on the redshift dependence of ω described by the first (left) and second (right) parameterizations, respectively. The regions blancked out in purple are ruled out by supernova constraints and the green regions are ruled out by WMAP [23]. Shaded areas are holographic constraints we obtained from the small l CMB spectrum. They have overlaps with the constraints gotten in [23].

With the more precise values for the supression region and a related better shape of the spectrum for low- l , the shaded area will be reduced and the holographic constraints from the cosmic duality will become tighter.

In order to get a better insight, we have shown in Fig.3 the allowed values of $\omega(z)$ as a function

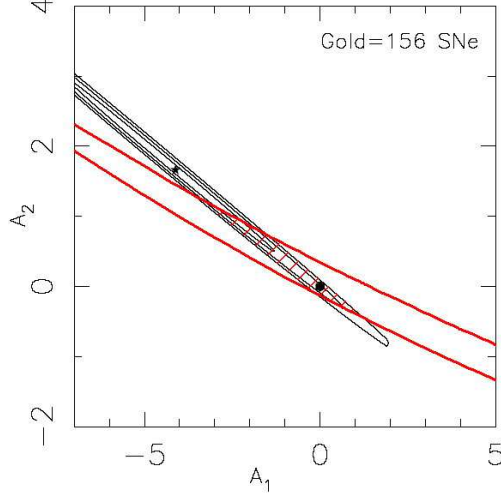


Figure 4: The constraint on the parameters A_1 and A_2 for the model Eq.(9). The area enclosed by the black curves is allowed by supernova data[25]. The red shaded area is the overlap of constraints from supernova and small l CMB observations.

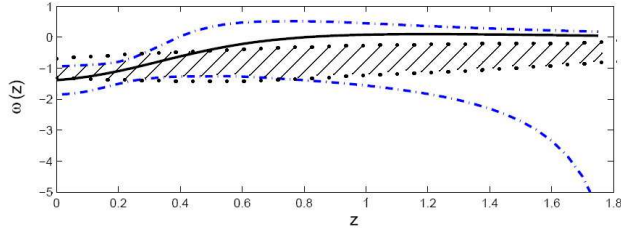


Figure 5: The evolution behavior of the parametrization Eq.(9). The area between the blue dot-dashed lines are the constraints from supernova data. The solid black line stands for the evolution of the golden set [24]. The black dotted lines are obtained from small l CMB observation. The shaded area is the overlap of supernova and low l CMB constraints.

of redshift z with supernova data [24] (blue dotted dash lines) and the small l CMB data (black dotted lines). The solid black lines stand for the evolution of the golden set of supernova data [24]. The left panel shows the result for the first parametrization. In contrast with the supernovae results, the correlation between the dark energy and small l CMB spectrum puts $\omega_1 + \omega_0$ well below zero. Thus the dark energy density did not dominate over the matter density at high z , from CMB observation. The shaded area is the combined constraint from the supernovae and small l CMB data. Including the low- l CMB constraint, the first parameterization cannot be ruled out as a choice of modelling dynamic dark energy even at high z . The right panel in Fig.3 exhibits the

behavior of $\omega^{II}(z)$ for the second parametrization. It is clear from both the supernovae and CMB constraints that the matter density did dominate over the dark energy density at high z in this parametrization.

We now investigate the third Ansatz for the redshift dark energy dependence. Fig.4 shows the relation of A_2 and A_1 . The area enclosed by the black curves is allowed by supernova observation[25]. The red shaded area is the overlap of the combined supernova and small l CMB suppression where the cutoff position is within the interval $3.8 \leq l_c \leq 4.2$. It leads to tighter constraints on the model. The behavior of the evolution of such a dark energy Ansatz is shown in Fig.5, where the blue dotted dash lines stem from the supernova data [24] and black dotted lines from low- l CMB data. The solid line stands for the evolution of the golden set of supernova data. It is clear that using the cosmic duality scenario the small l CMB spectrum puts tighter constraint on the evolution of ω .

In summary, we have employed the holographic cosmic duality to study the nature of the dark energy. Using the cosmic IR/UV duality, we obtained the quantitative agreement of low l CMB features to WMAP observation, which shows the effectiveness of the holohraphic idea. By the correlation disclosed between the dark energy and small l CMB power spectrum, we have obtained constraints on dark energy models from the low l CMB data. For the static equation of state, we have got the consistent range of ω with that from supernova experiment. This shows again the correctness of the idea of holographic cosmic duality. We have also studied constraints for the dynamic dark energy model and compared the results obtained from supernova data. To obtain more precise constraints on the dark energy through this holographic cosmic duality and to answer the question whether IR cutoff is exactly the future event horizon, exact location of the suppression position and precise shape of the CMB power are crucial, especially employing independent methods such as baryonic oscillations in future surveys [26].

Acknowledgments

This work was partially supported by NNSF of China, Ministry of Education of China, Ministry of Science and Technology of China under grant NKBRSG19990754 and Shanghai Education Commission. E. Abdalla's work was partially supported by FAPESP and CNPQ, Brazil. R.K.

Su's work was partially supported by the National Basic Research Project of China.

- [1] C.L. Bennett, et.al., *ApJS* **148** (2003) 1, astro-ph/0302214
D.N. Spergel, et.al., *ApJS* **148** (2003) 175, astro-ph/0302209
- [2] A. Berera, L. Z. Fang and G. Hinshaw, *Phys. Rev. D* **57** (1998) 2207; C. R. Contaldi, M. Peloso, L. Kofman and A. Linde, *JCAP* **0307** (2003) 002; J. M. Cline, P. Crotty and J. Lesgourgues, *JCAP* **0309** (2003) 010; M. Bastero-Gil, K. Freese and L. Mersini-Houghton, *Phys. Rev. D* **68** (2003) 123514; Y. S. Piao, S. Tsujikawa and X. Zhang, *Class. Quant. Grav.* **21** (2004) 4455.
- [3] J. P. Uzan, U. Kirchner and G. F. R. Ellis, *Mon. Not. Roy. Astron. Soc.* **344** (2003) L65; A. Linde, *JCAP* **0305**, (2003) 002; M. Tegmark, A. de Oliveira-Costa and A. Hamilton, *Phys. Rev. D* **68**, (2003) 123523.
- [4] G. Efstathiou, *Mon. Not. Roy. Astron. Soc.* **343**, (2003) L95.
- [5] J. P. Luminet, J. Weeks, A. Riazuelo, R. Lehou and J. Uzan, *Nature* **425** (2003) 593.
- [6] K. Enqvist and M. S. Sloth, *Phys. Lett.* **93**, (2004) 221302 hep-th/0406019; K. Enqvist, S. Hannestad and M. S. Sloth, astro-ph/0409275.
- [7] G. 't Hooft, *Salamfest 1993:0284-296* (QCD161:C512:1993), gr-qc/9310026; L. Susskind, *J. Math. Phys.* **36** (1995) 6377.
- [8] W. Fischler and L. Susskind, SU-ITP-98-39, UTTG-06-98, hep-th/9806039.
- [9] N. Kaloper and A. Linder, *Phys. Rev. D* **60** (1999) 103509; R. Easther and D. A. Lowe, *Phys. Rev. Lett.* **82** (1999) 4967; R. Brustein, *Phys. Rev. Lett.* **84** (2000) 2072; R. Brustein, G. Veneziano, *Phys. Rev. Lett.* **84** (2000) 5695; R. Bouusso, *JHEP* **7** (1999) 4, *ibid* **6** (1999) 28, *Class. Quan. Grav.* **17** (2000) 997; B. Wang, E. Abdalla, *Phys. Lett. B* **466** (1999) 122, **471** (2000) 346; B. Wang, E. Abdalla and R. K. Su, *Phys. Lett. B* **503**, (2001) 394.
- [10] G. Veneziano, *Phys. Lett. B* **454** (1999) 22; G. Veneziano, *CERN-TH/99-176* hep-th/9907012; E. Verlinde, hep-th/0008140.
- [11] R. Tavakol, G. Ellis, *Phys. Lett. B* **469** (1999) 37.
- [12] B. Wang, E. Abdalla and T. Osada, *Phys. Rev. Lett.* **85** (2000) 5507.
- [13] I. Savonijie and E. Verlinde, *Phys. Lett. B* **507** (2001) 305; Bin Wang, Elcio Abdalla and Ru-Keng Su, *Mod. Phys. Lett. A* **17** (2002) 23; S. Nojiri and S. D. Odintsov, *Int. J. Mod. Phys. A* **16** (2001) 3237; D. Kutasov, F. Larsen, *JHEP* **0101** (2001) 001, hep-th/0009244; F. Lin, *Phys. Lett. B* **507** (2001) 270; R. Brustein, S. Foffa and G. Veneziano, *Nucl. Phys. B* **601** (2001) 380; D. Klemm, A. C. Petkou and G. Siopsis, hep-th/0101076; R. G. Cai, *Phys. Rev. D* **63** (2001) 124018 hep-th/0102113; D. Birmingham and S. Mokhtari, *Phys. Lett. B* **508** (2001) 365 hep-th/0103108.
- [14] E. Witten, *Science* **285**, (1999) 512.
- [15] P. Horava and D. Minic, *Phys. Rev. Lett.* **85**, (2000) 1610.

- [16] T. Banks and W. Fischler astro-ph/0307459; B. Wang and E. Abdalla, *Phys. Rev.* **D69** (2004) 104014, hep-th/0308145; R. G. Cai, *JACP* **0402** (2004) 007; D. A. Lowe and D. Marolf, *Phys.Rev.* **D70** (2004) 026001 hep-th/0402162.
- [17] M. Li, *Phys. Lett.* **B603** (2004) 1, hep-th/0403127; Q. G. Huang and M. Li, *JCAP* **0408** (2004) 006 astro-ph/0404229.
- [18] S. D. H. Hsu, *Phys. Lett.* **B 594** (2004) 13 (hep-th/0403052); B. Wang, E. Abdalla and R. K. Su, hep-th/0404057; Y. Gong, *Phys. Rev. D* 70 (2004) 064029; K. Ke and M. Li, hep-th/0407056; S. Hsu and A. Zee, hep-th/0406142.
- [19] A. Cohen, D. Kaplan and A. Nelson, *Phys. Rev. Lett.* **82** (1999) 4971 hep-th/9803132.
- [20] D. A. Dicus and W. W. Repko, *Phys. Rev.* **D70** (2004) 083527, astro-ph/0407094
- [21] M. Chevallier and D. Polarski, *Int. J. Mod. Phys. D* **10** (2001) 213; E.V. Linder, *Phys. Rev. Lett.* **90**, (2003) 91301 astro-ph/0402503.
- [22] T.R. Choudhury and T. Padmanabhan, accepted by *A&A* astro-ph/0311622.
- [23] H.K. Jassal, J.S. Bagla and T. Padmanabhan, Final version to appear in *MNRAS* (Letters) astro-ph/0404378.
- [24] Gong Yungui, astro-ph/0405446.
- [25] Adam G. Riess et. al., *ApJ* **607** (2004) 665 astro-ph/0402512; U. Alam, V. Sahni, T.D. Saini and A.A. Starobinsky, *Mon. Not. Roy. Astron. Soc.* **354** (2004) 275 astro-ph/0311364; U. Alam, V. Sahni and A.A. Starobinsky, *JCAP* **0406** (2004) 008 astro-ph/0403687.
- [26] Filipe B. Abdalla and S. Rawlings *Mon. Not. Roy. Astron. Soc.* astro-ph/0411342.